J Pharmacol Sci **101**, 66 – 76 (2006)

Journal of Pharmacological Sciences

Full Paper

A Critical Role of TRPM2 in Neuronal Cell Death by Hydrogen Peroxide

Shuji Kaneko[1,*], Seiko Kawakami[1], Yuji Hara[2], Minoru Wakamori[2], Etsuko Itoh[1], Toshiyuki Minami[1], Yuki Takada[3], Toshiaki Kume[3], Hiroshi Katsuki[3], Yasuo Mori[2], and Akinori Akaike[3]

[1]*Department of Molecular Pharmacology and* [3]*Department of Pharmacology, Graduate School of Pharmaceutical Sciences, Kyoto University, Sakyo-ku, Kyoto 606-8501, Japan*
[2]*Laboratory of Molecular Biology, Graduate School of Engineering, Kyoto University, Nishigyo-ku, Kyoto 615-8510, Japan*

Received February 2, 2006; Accepted March 13, 2006

Abstract. A brief exposure to hydrogen peroxide (H_2O_2) induces severe deterioration of primary cultured neurons in vitro. We have investigated a link between the H_2O_2-induced neuronal death and Ca^{2+}-permeable TRPM2 channels regulated by ADP-ribose (ADPR). In cultured cerebral cortical neurons from fetal rat, TRPM2 proteins were detected at cell bodies and neurite extensions. Application of H_2O_2 to the cultured neurons elicited an increase in intracellular Ca^{2+} concentration ($[Ca^{2+}]_i$) caused by Ca^{2+} influx and the Ca^{2+}-dependent neuronal death in a similar concentration range. Molecular cloning of TRPM2 cDNA from rat brain revealed several differences in amino acid sequences within the Nudix box region as compared with those of human and mouse TRPM2. ADPR-induced current responses, H_2O_2-induced Ca^{2+} influx, and H_2O_2-induced cell death were induced in human embryonic kidney cells heterologously expressing rat TRPM2. Treatment of cultured neurons with small interfering RNA against rat TRPM2, which efficiently suppressed immunoreactive TRPM2 content and the H_2O_2-induced Ca^{2+} influx, significantly inhibited H_2O_2-induced neuronal death. These results suggest that TRPM2 plays a pivotal role in H_2O_2-induced neuronal death as redox-sensitive Ca^{2+}-permeable channels expressed in neurons.

Keywords: ADP-ribose, cation channel, calcium homeostasis, cerebral cortex, TRP channel

Introduction

A variety of neurodegenerative disease states have been associated with oxidative damage. Such stress is thought to be mediated by excessive exposure of cells to reactive oxygen/nitrogen species, which can be generated by ischemia/reperfusion, glutamate overflow, *β*-amyloid peptides, neurotoxins, oxidative burst as part of immune response, or by the presence of free transition metal ions (1 – 5). Hydrogen peroxide (H_2O_2) is a stable and freely diffusable form of reactive oxygen species (ROS) normally produced in living cells including neurons. Substantial evidences indicate etiological links between generation of H_2O_2 and neurodegenerative diseases (6). Exposure to H_2O_2 induced both apoptotic-like delayed neuronal death and necrosis in cultured neurons (7), which are mediated by rise in intracellular Ca^{2+} concentration ($[Ca^{2+}]_i$), mitochondrial dysfunction, and activation of poly(ADP-ribose) polymerase (PARP) responding to DNA damage (8, 9). Recently, the rise in $[Ca^{2+}]_i$ by H_2O_2 has been ascribed to the activation of non-selective cation channels in striatal neurons (10), which may lead to irreversible depolarization and unregulated Ca^{2+} entry followed by neuronal death (6, 11).

Several members of the TRP superfamily channels are regulated by intracellular conditions including redox states (12). One of them, TRPM2, formerly known as TRPC7 or LTRPC2, is an ADP-ribose (ADPR)-gated Ca^{2+}-permeable, nonselective cation channel having a putative ADPR-recognizing Nudix box motif in the intracellular C-terminal tail (13, 14). TRPM2 is highly expressed in the brain (15, 16) and in immune cells of the monocytic lineage (13, 14). In the brain, TRPM2 is expressed in activated microglial cells and functions as a Ca^{2+} entry pathway triggered by H_2O_2 and ADPR, while in situ hybridization data rather indicated the expression

*Corresponding author. skaneko@pharm.kyoto-u.ac.jp
Published online in J-STAGE: April 29, 2006
DOI: 10.1254/jphs.FP0060128

of TRPM2 mRNA throughout the mouse brain including neurons (17). In the present study, we investigated the expression of TRPM2 in cultured cortical neurons and possible involvement of the non-selective cation channel in H_2O_2-induced Ca^{2+} influx and cell death using cDNA cloning and gene silencing by small interfering RNA (siRNA) techniques.

Materials and Methods

Cortical cultures

Primary cultures of cortical neurons were obtained from E17-E19 Wistar rat embryos according to the procedures published previously (18). In brief, single cells mechanically isolated from cerebral cortices of fetal rats were plated directly on Falcon 60-mm dishes (for cell viability assay) or on polyethyleneimine-coated glass coverslips that were placed in 60-mm dishes or 12-well plates (for immunostaining and Ca^{2+} imaging). Cultures were incubated in Eagle's minimal essential salt medium (Eagle's MEM) supplemented with 2 mM L-glutamine, 11 mM glucose, 24 mM $NaHCO_3$, 10 mM HEPES, pH 7.4, and 10% heat-inactivated fetal bovine serum (1 – 8 days after plating) or 10% heat-inactivated horse serum (after 9 days from plating). Growth of non-neuronal cells was suppressed by addition of 10 μM cytosine arabinoside after 7 days of plating. Mature cultures were used at 9 – 14 days in vitro (DIV). When gene expression efficacy was tested, cultures were transfected with plasmid encoding EGFP and Lipofectamine 2000 at 5 DIV and incubated for 1 – 2 days.

Cell line culture and transfection

Human embryonic kidney (HEK) 293 and tsA-201 cells were grown to 80% confluence in Dulbecco's modified Eagle's medium supplemented with 10% fetal bovine serum and 0.06% kanamycin. Cells were split and plated on glass coverslips at 10% confluence 12 h before transfection. The medium was renewed immediately before transfection with rTRPM2 /pcDNA3z (1 – 2 μg plasmid/60-mm dish) with Lipofectamine 2000 (Invitrogen, Carlsbad, CA, USA). The cells were maintained at 37°C for at least 18 h before Ca^{2+} imaging, immunostaining, Western blotting, current recording, and cell viability assays.

Molecular cloning of rat TRPM2

A rat brain TRPM2 gene was cloned by RT-PCR according to the similarity of human (NM_003307) and mouse (NM_138301) TRPM2 cDNA sequences to those of a rat genome contig (NW_043433) and an annotated TRPC7-like gene (LOC294329). Poly(A)$^+$mRNA was extracted from 3-week-old rat cerebral cortices by the guanidium/CsCl method followed by oligo(dT)-cellulose column selection. Single-strand DNA was synthesized with a primer (5'-tcagaagtgagcgccaaacagc-3') by reverse transcriptase XL from avian myeloblastosis virus (Takara Bio, Ohtsu). PCR reaction was performed for 35 cycles at an annealing temperature of 60°C by the Expand High Fidelity PCR system (Roche Diagnostics, Indianapolis, IN, USA) with another PCR primer (5'-ctctcctctggtggatctgg-3'). A 4.6-kb product was extracted from agarose gel, inserted into pGEM-T easy vector (Promega, Madison, WI, USA) and sequenced. The nucleotide sequences of two independent PCR products completely matched each other and deposited to Genbank (AB193179). The full length of rat TRPM2 was subcloned into pcDNA3.1/Zeo vector (Invitrogen) to yield a plasmid rTRPM2/pcDNA3z.

Immunostaining

Two rabbit polyclonal antibodies, M2-C and M2-Nudix, were raised against conjugated peptides corresponding to specific C-terminal regions of mouse TRPM2 (amino acid sequences: (C)KENYLQNQQY-QQKQRPEQK at 1126 – 1144 and (C)GSREPGEMLP-RKLK at 1387 – 1400). Cells on coverslips were fixed with 4% paraformaldehyde in phosphate-buffered saline (PBS) for 30 min at room temperature, washed three times with PBS, and permeabilized for 15 min with 0.2% Trixon X-100 in PBS. The cells were incubated overnight at 4°C with PBS containing one or two of the following antibodies: anti-mouse TRPM2 antibody (1:300 – 3000 dilution), anti-MAP2 antibody (1:400 dilution, M-1406; Sigma, St. Louis, MO, USA), an anti-GAPDH antibody (1:30000 dilution; Ambion, Austin, TX, USA), anti-GFAP antibody (1:50 dilution, Sigma). For immunofluorescnence analysis, Alexa Flour 488-labeled goat anti-rabbit IgG and/or Alexa Fluor 568-labeled anti-mouse IgG (Molecular Probes, Eugene, OR, USA) was used at 1:200 dilution as the second antibody for visualization with a laser scanning confocal imaging system (MRC-1024; Bio-Rad Laboratories, Hercules, CA, USA). In 3,3'-diaminobenzidene (DAB) staining, the cells were visualized with the ABC system (Vector Laboratories, Burlingame, CA, USA) and DAB. The coverslips were mounted with Vectashield (Vector Lab) on slides and photographed under a Nikon TE300 microscope with a Coolpix E4500 digital camera.

Western blotting

Membrane pellets were obtained from cells by brief centrifugation and lysed with a lysis buffer (50 mM Tris-HCl, 150 mM NaCl, 1% Triton X-100, 3 mM EDTA, 20 μg/ml aprotinin, 2 mM PMSF, pH 7.4). An aliquot of lysate was added to an equal volume of sample buffer

(124 mM Tris-HCl, pH 6.8, 10% glycerol, 4% SDS, 4% 2-mercaptoethanol, 0.02% bromophenol blue) and loaded on a 7% SDS-polyacrylamide gel. Proteins were blotted onto Immobilon-P PVDF transfer membranes (Millipore, Billerica, MA, USA). After incubation with blocking solution for 1 h, the membranes were incubated overnight at 4°C with the appropriate primary antibody diluted in blocking solution. After three washes, membranes were incubated for 1 h at room temperature with either anti-mouse IgG horseradish peroxidase-conjugated whole sheep antibody or anti-rabbit IgG. After three washes, specific bands were detected by ECL (Amersham Pharmacia Biotech, Piscataway, NJ, USA). Blots were exposed to Fuji X-ray film, and the image was digitized by an image scanner.

Ca^{2+} imaging

Intracellular Ca^{2+} concentration was measured with the fluorescent Ca^{2+} indicator fura-2 acetoxymethyl ester (fura-2 AM; Dojindo, Kumamoto). Cells on glass coverslips were incubated for 30 min at 37°C in HEPES-buffered saline containing 5 μM fura-2AM. After rinsing with HEPES buffer, the coverslip was mounted on the recording chamber of a Nikon fluorescent microscope equipped with an ARGUS-HiSCA imaging system (Hamamatsu Photonics, Shizuoka). The recording chamber was initially perfused with HEPES buffered saline at a flow rate of 1 ml/min, and test solutions were applied by switching the perfusion line. The fluorescent image at 500 nm was scanned at an interval of 5 s with alternative excitation at 340 and 380 nm at room temperature and stored in a computer with Aquacosmos imaging software (Hamamatsu Photonics). The fluorescence ratio ($F_{340/380}$) within an image area of an individual cell was calculated.

Electrophysiology

Whole-cell currents were recorded at room temperature with an Axopatch 200B amplifier (Axon Instruments, Union City, CA, USA). Currents were sampled and analyzed with pCLAMP 6.02 software (Axon). Patch pipettes were made from borosilicate glass capillaries (1.5-mm outer diameter; Hilgenberg, Malsfeld, Germany) using a P-97 micropipette puller (Sutter Instruments, Novato, CA, USA) and the resistance ranged from 2 to 4 Mohm when filled with the pipette solution (105 mM CsOH, 105 mM aspartic acid, 40 mM CsCl, 1.3 mM $CaCl_2$, 2 mM $MgCl_2$, 5 mM EGTA, 2 mM ATP2Na, 5 mM HEPES, pH 7.25 with CsOH, and calculated [free-Ca^{2+}] was 50 nM). Rapid change of external solution was made by a modified "Y-tube" method. The recording solution was 125 mM NaCl, 2 mM $CaCl_2$, 1.2 mM $MgCl_2$, 10 mM glucose, 51 mM mannitol, 11.5 mM HEPES, pH 7.4 with NaOH. Nominally Ca^{2+}-free solution contained 121.7 mM NaCl, 1.2 mM $CaCl_2$, 1.2 mM $MgCl_2$, 2 mM EGTA, 10 mM glucose, 51 mM mannitol, 11.5 mM HEPES, pH 7.4 (90 nM [free-Ca^{2+}]).

Cell viability assay

Toxicity of H_2O_2 on cultured neurons and HEK cells was assessed by the trypan blue exclusion method (18). After exposure to drugs in Eagle's MEM at 37°C for the indicated period, cells were immediately stained with 1.5% Trypan blue for 10 min at room temperature, fixed with ice-cold, isotonic formalin (pH 7.0), and rinsed with physiological saline. The viability of the culture was estimated as the percentage of the ratio of the number of unstained, viable cells to the total number of stained and unstained cells. Over 100 cells per coverslip were counted in determining the viability, and at least 5 coverslips were used for one treatment. Dilution of H_2O_2 was made fresh from 30% solution (Wako, Osaka) just prior to experiments.

siRNA treatment

An siRNA targeted to 168 – 188 base downstream to the start codon ATG of rat TRPM2 was synthesized by Silencer siRNA construction kit (Ambion) with the following primers: 5'-aaacacgtccatgagatgcctcctgtctc-3' (for antisense strand) and 5'-aaaggcatctcatggacgtgtcctgt ctc-3' (for sense strand). Cultured neurons were transfected at 5 – 6 DIV with the siRNA at a concentration ranging 0.1 – 10 nM by Lipofectamine 2000 for 4.5 h in Opti-MEM solution (Invitrogen). As the control, an siRNA to GAPDH was synthesized according to the instructions of the siRNA construction kit and used at a final concentration of 3 nM.

Statistics

Data are shown as the means ± S.E.M.s. Prism 4 (GraphPad, San Diego, CA, USA) was used for ANOVA with the *post hoc* Tukey test.

Results

Expression of TRPM2 in rat cortical neurons

First we have characterized the neuronal cultures by triple staining for nuclear DNA, a neuronal marker, MAP2, and an astroglial marker, GFAP (Fig. 1a). Most of the large, round cells with thick cell bodies and long extensions were MAP2-positive neurons and consisted of >70% of the total cell number identified by nuclear staining with DAPI. The remaining cells were GFAP-positive astrocytes with flat cell bodies and stellate morphology, whose number was not increased after

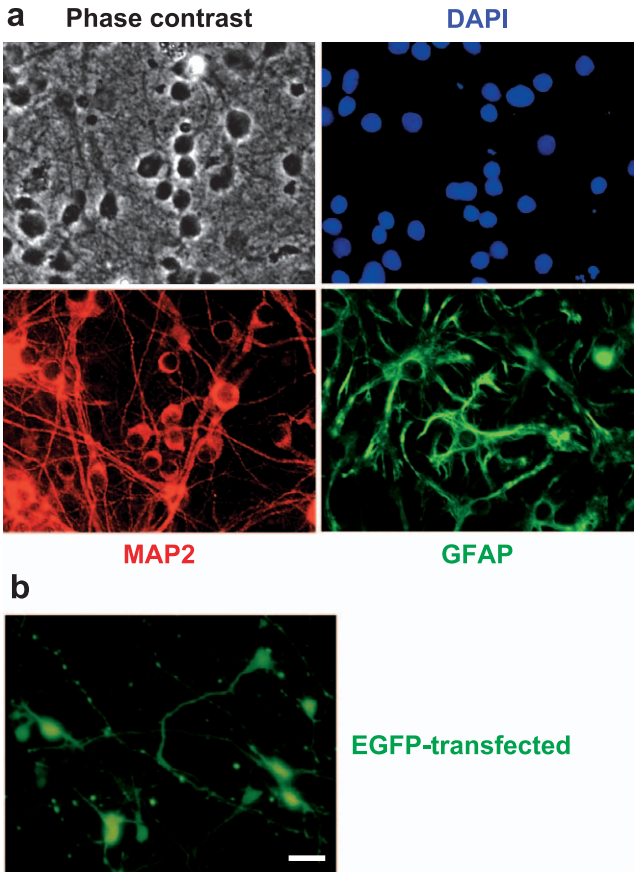

Fig. 1. Morphology of dissociated cortical cultures at 10 DIV. Cells were mechanically dissociated from cerebral cortex of fetal rats (E19), cultured, and treated once with 10 μM cytosine arabinoside at 7 DIV. a: Triple staining of cultured cells for nuclear DNA with DAPI, neuronal MAP2, and astroglial GFAP. Four images were taken from the identical region of a coverslip. b: Heterologous expression of EGFP in cultured neurons. Neuronal culture was transfected with plasmid containing cDNA for EGFP at 5 DIV and incubated for 48 h. Scale bar = 20 μm.

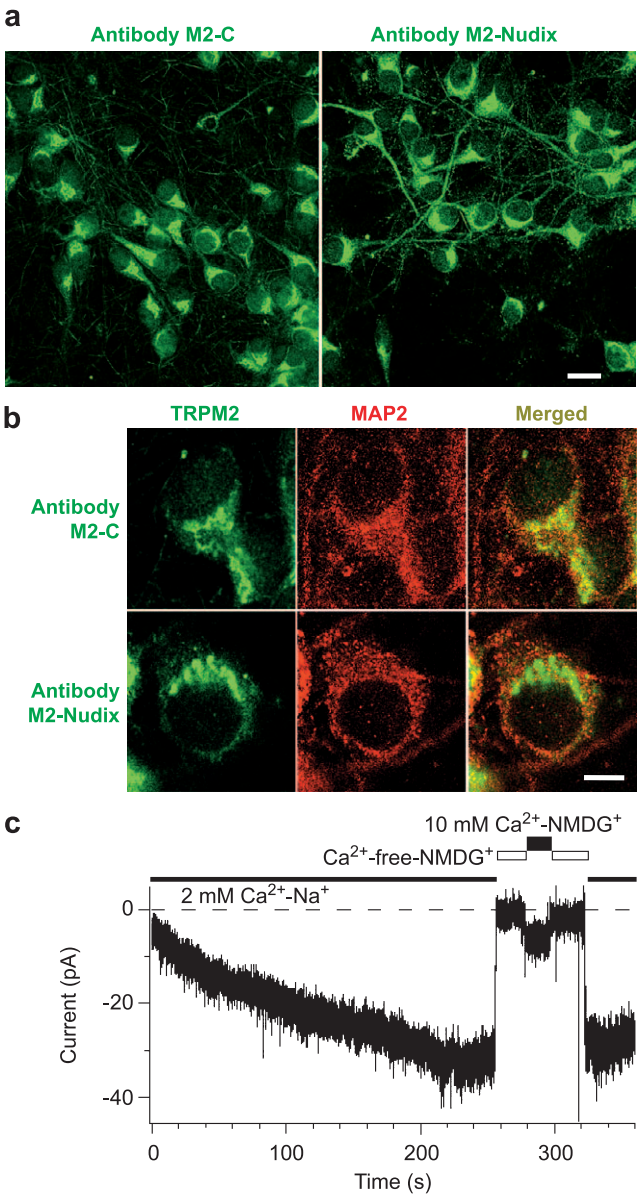

Fig. 2. Expression of TRPM2 in cultured cerebral cortical neurons from fetal rats at 13 DIV. a: Two anti-TRPM2 antibodies, M2-C and M2-Nudix, were used for confocal immunofluorescence microscopy. Scale bar = 20 μm. b: Subcellular localization of TRPM2-immunoreactivity in MAP2-positive neurons. Scale bar = 10 μm. c: ADPR-induced cation current in cortical neuron acutely dissociated from 20- to 25-day-old rats. One millimolar ADPR was included in the patch pipette.

treatment with the cytosine arabinoside at 7 DIV. One to two days after transfection with plasmid containing cDNA for EGFP at 5 DIV, green fluorescence was observed in 40.4 ± 6.8% (n = 12) of neurons with long dendrites after 1 – 2 days (Fig. 1b), indicating successful transgene expression in cultured cortical neurons.

Expression of TRPM2 in rat neurons were evaluated using two kinds of anti-TRPM2 antibodies directed against different C-terminal regions of mouse TRPM2. With both antibodies, TRPM2-immunoreactivity was observed in most (>90%), but not all, of the cultured neurons. The staining with anti-TRPM2 antibodies were observed in cell bodies and neurites of neurons (Fig. 2a). In high-magnification images, the TRPM2-immunoreactivity was distributed to plasma membranes and intracellular membraneous particles of MAP2-positive cells (Fig. 2b). The expression of TRPM2 was much lower in premature neurons at 2 – 4 DIV and never colocalized with GFAP-positive cells at any DIV (data not shown).

To confirm the expression of functional TRPM2 channels on the cell surface of neurons, we have recorded the ADPR-induced current response from cortical neurons acutely isolated from young rats (Fig. 2c) since cultured neurons had many neurites and

cell-to-cell contacts that would interfere with patch-clamp analysis. When the dissociated rat cortical neurons were dialyzed with the pipette solution containing 1 mM ADPR, inward currents developed gradually and reached a peak at 4 – 6 min in 5 out of 6 neurons, whereas 2 out of 6 neurons showed inward currents in the absence of ADPR. The average of peak inward current amplitudes was 21.3 ± 5.7 pA with ADP-ribose and 5.9 ± 4.1 pA without ADPR (P<0.05) at a holding potential of −60 mV. The inward currents completely disappeared by omission of both Ca^{2+} and Na^{+} from the external solution, whereas addition of 10 mM Ca^{2+} partially restored the currents, suggesting that Ca^{2+}-permeable cation channels are opened by intracellular ADPR in cortical neurons.

H_2O_2-induced cell death and Ca^{2+} influx in cultured cortical neurons

Cultured cortical neurons are vulnerable to H_2O_2 and cause cell death after application of H_2O_2 (8, 19, 20). As a first step toward understanding the role of Ca^{2+}-permeable TRPM2 in the pathology of H_2O_2 in neurons, we have compared the toxic effects of H_2O_2 on rat cortical neurons in the presence and absence of Ca^{2+}, with reference to the excitotoxic effects of glutamate (Glu) via activation of Ca^{2+}-permeable NMDA channels (21). Treatment of cultures for 1 h with 500 μM Glu caused significant decrease in the number of living cells as indicated by the increase in the stained neurons in the Trypan blue exclusion assay, which was restored under the Ca^{2+}-free condition (Fig. 3). Treatment of cultures with 1 mM H_2O_2 caused prominent neuronal death within 20 min, which was significantly (P<0.01), but not completely, inhibited in the absence of extracellular Ca^{2+}, indicating that Ca^{2+} plays substantial role in the H_2O_2-induced neuronal death. Lower concentrations of H_2O_2, requiring longer period of incubation, also caused neuronal death (data not shown). Minimum degenerative concentration of H_2O_2 was 30 μM for 8-h incubation, in which 60.5 ± 5.9% (n = 20) cells were dead, suggesting that cultured cortical neurons are vulnerable to H_2O_2 with equivalent sensitivity of cultured striatal neurons in vitro (22) which are thought to be particularly sensitive to H_2O_2 (23, 24).

To explore the relationship between acute Ca^{2+} influx and neuronal death by H_2O_2, we measured H_2O_2-induced changes in $[Ca^{2+}]_i$ using fura-2 fluorometry. In comparison with the immediate increase in $[Ca^{2+}]_i$ after Glu exposure (Fig. 4a), application of 1 mM H_2O_2 caused a synchronously-bursting increase in $[Ca^{2+}]_i$ after several minutes of delay in Ca^{2+}-containing solution (Fig. 4b). The plateau level of $F_{340/380}$ ratio after 12-min treatment with Glu and H_2O_2 was 1.29 ± 0.24 (n = 47) and

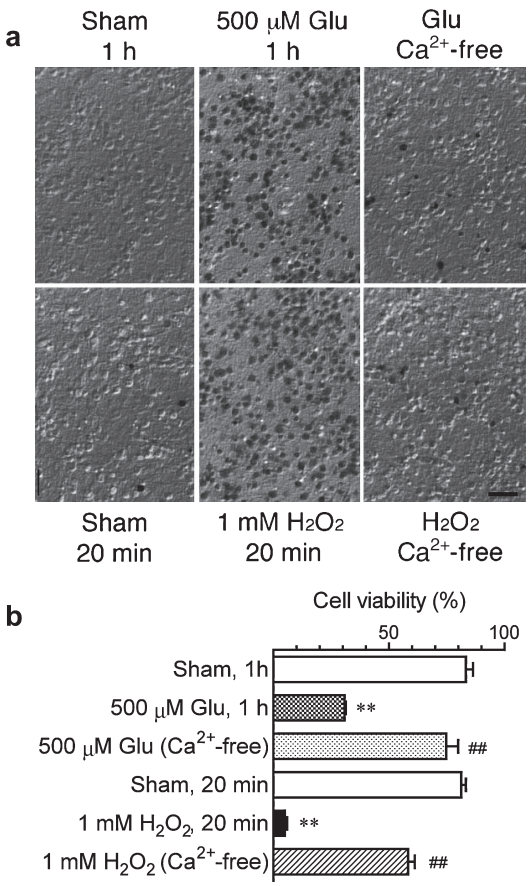

Fig. 3. Requirements of extracellular Ca^{2+} in the vulnerabilities of cultured neurons to glutamate (Glu) and H_2O_2. a: Tripan blue staining of neuronal cultures after treatment at 37°C in either normal or Ca^{2+}-free medium containing 500 μM Glu or 1 mM H_2O_2. Sham treatment was done in the Ca^{2+}-free medium for the indicated period. b: Cell viabilities were calculated from the numbers of stained and non-stained neurons in 5 independent experiments. **, P<0.01 *vs* Sham group and $^{\#\#}$, P<0.01 *vs* treated group by one-way ANOVA with the *post hoc* Tukey test. Scale bar = 50 μm.

1.25 ± 0.21 (n = 51), respectively, suggesting that these neurotoxins are equipotent in increasing $[Ca^{2+}]_i$. Perfusion of neurons for 4 – 5 min with Ca^{2+}-free solution per se did not evoke any store-related Ca^{2+} entry in neurons (Fig. 4c), and 5-min perfusion with 1 mM H_2O_2 under Ca^{2+}-free condition only elicited a subtle rise in $[Ca^{2+}]_i$ (Fig. 4d). However, re-addition of 2 mM Ca^{2+} in perfusing solution 5 min after washout of H_2O_2 evoked marked and sustained increase in $[Ca^{2+}]_i$ with less delay of onset. The average $F_{340/380}$ ratio at 12 min after application of H_2O_2 (2 min after addition of Ca^{2+}) was 1.45 ± 0.04 (n = 52). The H_2O_2-induced Ca^{2+} influx was dose-dependent and detectable at a minimum of 30 μM in the Ca^{2+}-addition protocol (Fig. 4e). Under this condition, the EC_{50} and Hill slope values were 546 nM (95% confidential limits = 421 – 709 nM, n = 6 – 10) and 1.7 ±

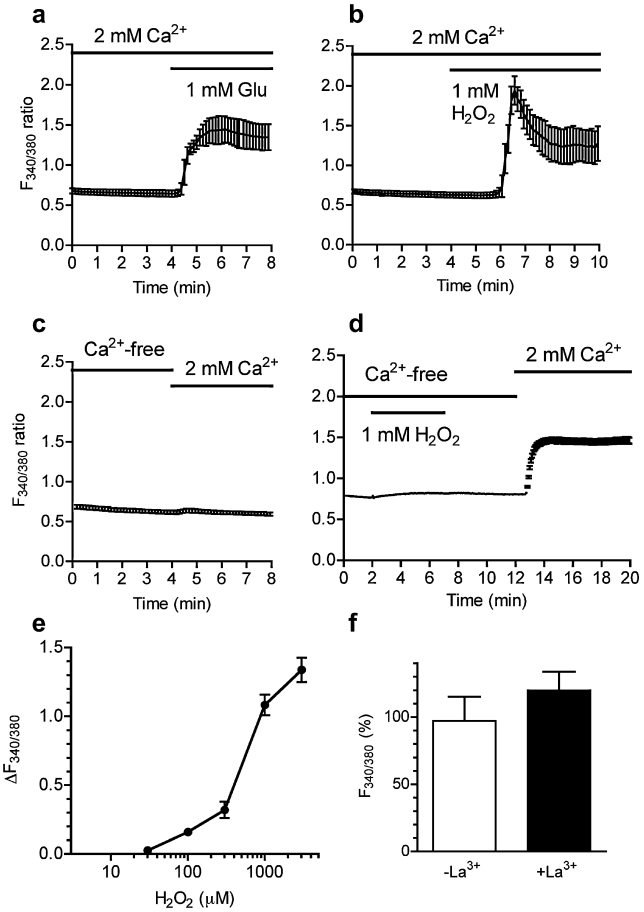

Fig. 4. H_2O_2-induced changes in $[Ca^{2+}]_i$ in cultured cerebral cortical neurons. To fura-2-loaded neurons, 1 mM glutamate (Glu) (a) or 1 mM H_2O_2 (b) was applied in the presence of extracellular Ca^{2+}. In different sets of experiments, neurons were perfused with Ca^{2+}-free solution, and 2 mM Ca^{2+} was added (c). Using this protocol, Ca^{2+} release and Ca^{2+} influx induced by H_2O_2 were discriminated (d), and concentration dependency of H_2O_2 for the Ca^{2+} influx was evaluated (e). The effect of La^{3+} was evaluated by adding 1 μM $LaCl_3$ to 2 mM Ca^{2+}-containing solution at 15 min in an experimental protocol identical to that used in panel d, and changes in OD ratio was monitored after 3 min (f) (n = 8).

0.3, respectively. Pharmacologically, the H_2O_2-induced Ca^{2+} influx was not inhibited but rather potentiated ($19.7 \pm 12.8\%$, $n = 8$) in the presence of 1 μM La^{3+} (Fig. 4f). These results suggest that the increase in $[Ca^{2+}]_i$ after H_2O_2 is largely mediated by Ca^{2+} influx via H_2O_2-activated Ca^{2+}-permeable channels and that the insensitivity to La^{3+} is distinct from the pharmacological sensitivity of La^{3+}-sensitive TRPC or voltage-dependent Ca^{2+} channels.

Molecular cloning and heterologous expression of rat TRPM2 cDNA

Human (NM_003307) and mouse (NM_138301) TRPM2 genes share 84.2% identity in the deduced amino acid sequences and 82.9% identity in the nucleotide sequences of open reading frame. Although the anti-mouse TRPM2 antibody recognized an immunoreactive substance in rat cortical neurons, we have cloned rat TRPM2 gene from rat brain cDNA library to study the channel function by heterologous expression and to manipulate expression of TRPM2 in cultured neurons by RNA interference (RNAi). In a draft sequence of rat genome (LOC294329), a putative TRPM2 gene was found, and the expression was supported by multiple EST sequences. RT-PCR amplification of cDNAs from both rat brain mRNA and mRNA purified from cultured cortical neurons yielded a 4.6-kb product. The rat TRPM2 gene encoded 1507 amino acids identically to mouse gene and share 94.5% amino acid identity with mouse TRPM2. However, several differences in the deduced amino acid sequences were found within the Nudix box region as compared with those of human and mouse TRPM2 (Fig. 5a). Glu^{1393} that is conserved among human and mouse TRPM2 and human NUDT9 was Lys in rat TRPM2. Two positively-charged residues of Arg^{1401} and Arg^{1404} in human and mouse TRPM2 were replaced to glutamines. These differences raised the possibility of a different mechanism of gating in rat TRPM2-forming channels. In Western analysis of HEK cells transfected with rat TRPM2 cDNA, a single 170-kD band was detected but not in mock-transfected control cells (Fig. 5b), confirming the integrity of cDNA and crossreactivity of anti-mouse TRPM2 antibody to rat TRPM2 protein.

To compare the sensitivities of rat and human TRPM2 channels to ADPR, we recorded whole-cell current responses of HEK cells after heterologous expression of rat or human TRPM2. In cells expressing rat TRPM2, dialyzation with patch pipette solution containing 30 μM ADPR elicited a slow-onset, inward current response at a holding potential of −50 mV (Fig. 5c). The I-V curve of ADPR-induced rat TRPM2 currents was linear with a reversal potential around 0 mV (Fig. 5d), similar to that of human TRPM2 channels. The ADPR-evoked response was reduced by omission of extracellular Ca^{2+} with EGTA (Fig. 5e), supportive of Ca^{2+}-dependent opening of TRPM2 channels (16, 25). A comparative experiment on the sensitivity to ADPR (Fig. 5f) revealed that the average current density of the rat TRPM2 channel response was significantly ($P<0.05$) higher than that of human channels at 30 μM ADPR and that the current amplitude or the proportion of responding cells was not different at lower or higher concentrations. These results suggest that rat TRPM2 channels are more sensitive to ADPR than human TRPM2 channels, while other properties are identical.

In a series experiment of fura-2 fluorescence and

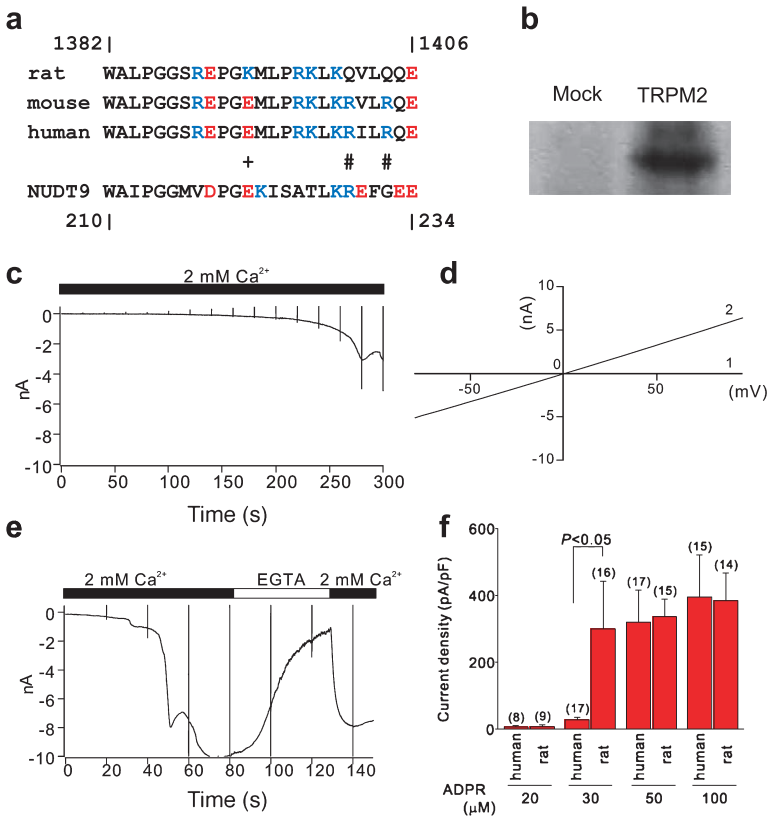

Fig. 5. Amino acid sequence and sensitivity of rat TRPM2 channel to ADPR. Multiple alignment of the Nudix motif region of mammalian TRPM2 genes (at amino acids 1382 – 1406 in rat TRPM2) with human NUDT9 indicates several differences in rat TRPM2 in comparison with human and mouse genes (a). A plus (+) symbol indicates a conversion of a negatively-charged residue (red character) to a positively-charged one (blue character), and # symbols indicate loss of positive charges in rat TRPM2. Heterologous expression of rat TRPM2 protein in HEK cells was confirmed by Western blot analysis (b). Typical whole-cell current responses were recorded from HEK cells expressing rat TRPM2 in the presence of 30 μM ADPR in the pipette solution (c). I-V relationship of TRPM2 currents were recorded before (trace 1) and after (trace 2) the delayed activation of TRPM2 channels with intracellular ADPR (100 μM, d). Decrease in the ADPR (100 μM)-induced cation current was observed by removal of extracellular Ca^{2+} with EGTA (e). Difference in the sensitivity to ADPR was compared at different ADPR concentrations between human and rat TRPM2 channels (f).

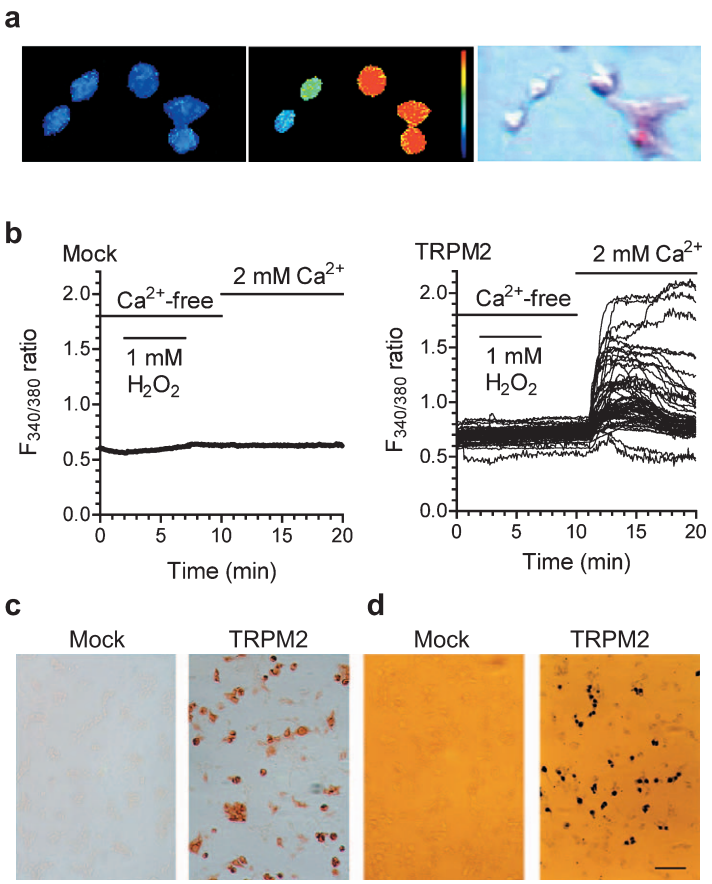

Fig. 6. Functional expression of rat TRPM2 in HEK cells. a: In the microscopic images in fura-2 fluorescence analysis (left panel), $OD_{340/380}$ ratio 5 min after treatment with 1 mM H_2O_2 was converted to spectoral pseudocolor (middle panel, from violet = 0 to red = 2). Following the fura-2 measurement, expression of TRPM2 was checked by immunostaining of TRPM2 with DAB (right panel). b: Application of 1 mM H_2O_2 to mock-transfected HEK cells gave no change in $[Ca^{2+}]_i$ (n = 53), whereas HEK cells transfected with rat TRPM2-carrying plasmid elicited H_2O_2-induced Ca^{2+} influx (indicated as individual traces from 55 cells). c: Efficacy of heterologous expression of rat TRPM2 in HEK cells are shown in the DAB-stained immunocytochemical image. d: A part of the HEK cells expressing rat TRPM2 died after treatment with 100 μM H_2O_2 at 37°C for 20 min, while mock-transfected cells were not affected. Scale bar = 50 μm.

subsequent immunostaining of the fura-2-loaded cells, H_2O_2-induced rise in fluorescence ratio by Ca^{2+} influx was observed in a portion of HEK cells transfected with rat TRPM2 cDNA, and TRPM2 immunoreactivity was detected in the identical population of cells (Fig. 6a). H_2O_2-induced Ca^{2+} influx was not observed in the mock-transfected HEK cells, while most of TRPM2-transfected cells caused Ca^{2+} influx after stimulation with H_2O_2 (Fig. 6b). In comparative experiments of immunostaining and H_2O_2-induced cell death, 42.1 ± 4.6% (n = 8) of TRPM2-transfected HEK cells were immunostained (Fig. 6c), while H_2O_2-induced cell death was observed in 34.0 ± 2.4% (n = 24) of sister cultures (Fig. 6d). These results indicate that heterologous expression of rat TRPM2 conferred both H_2O_2-induced Ca^{2+} influx and cell death in HEK cells.

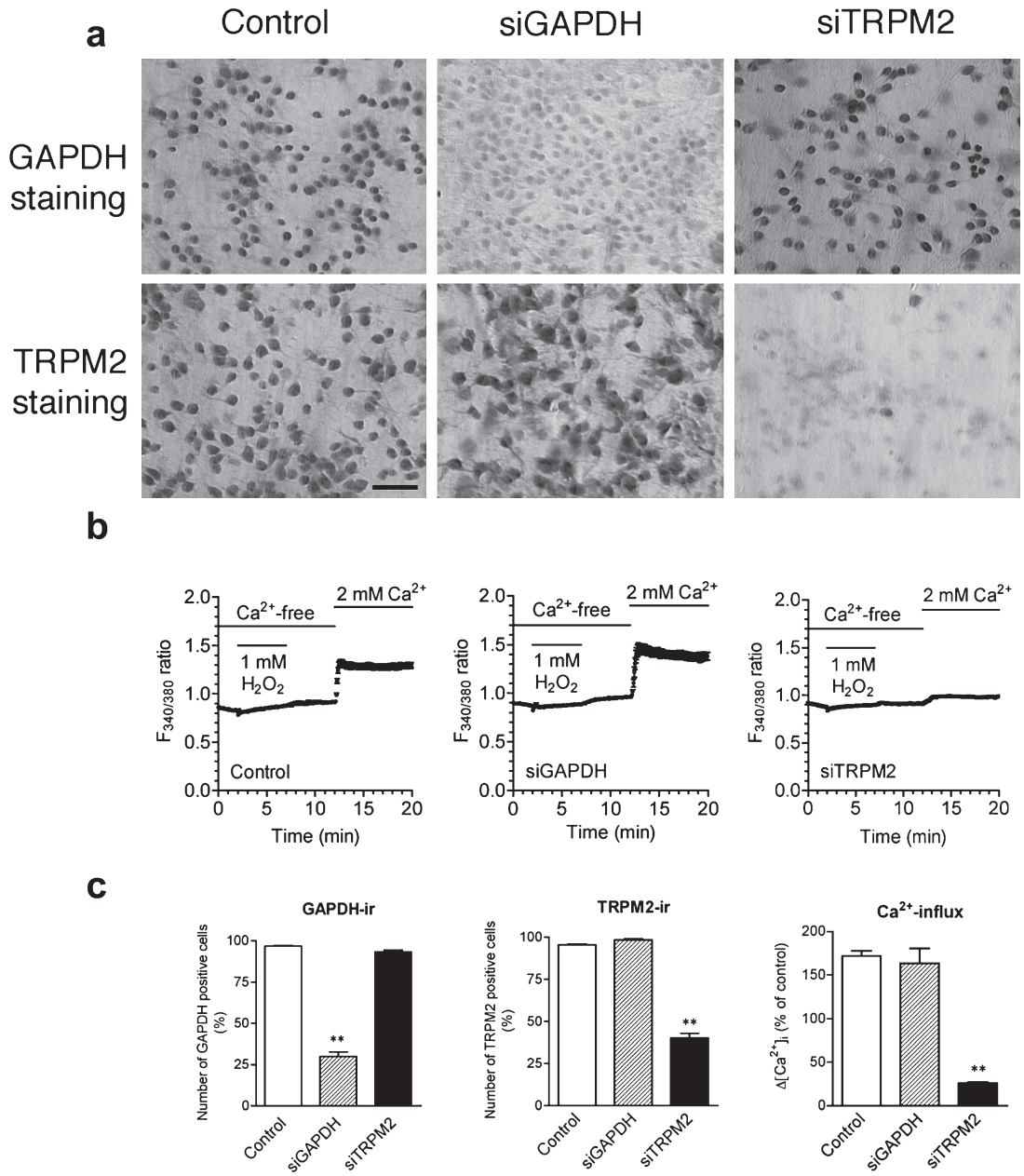

Fig. 7. Specific attenuation of TRPM2 immunoreactivity and H_2O_2-induced Ca^{2+} influx by siRNA silencing in cultured cortical neurons. a: Representative immunocytochemical DAB staining of neurons pretreated with or without (control) either siRNA for GAPDH (siGAPDH, 3 nM) or TRPM2 (siTRPM2, 1 nM). Scale bar = 50 μm. b: H_2O_2-induced changes in $[Ca^{2+}]_i$ was measured in fura-2-loaded neurons pretreated with lipofection reagent only (control, n = 45), siGAPDH (n = 27) or siTRPM2 (n = 52). c: Average effects of siGAPDH- and siTRPM2-induced silencing on the number of immune-positive neurons for GAPDH and TRPM2, and the H_2O_2-induced Ca^{2+} influx. **, P<0.01 *vs* control by one-way ANOVA with the *post hoc* Tukey test.

Gene silencing of TRPM2 in cultured cortical neurons

Nucleotide sequence of rat TRPM2 enabled targeted gene silencing of TRPM2 in cultured neurons. We tested several sets of siRNA targeted to specific nucleotide sequences of rat TRPM2 and found that treatment of neuronal culture with one of the siRNAs for TRPM2 (siTRPM2) at 1 nM reduced the intensity of staining and the number of immunoreactive cells after 3 – 4 days of transfection without affecting GAPDH staining and morphology of neurons (Fig. 7a). Conversely, a control siRNA for GAPDH (siGAPDH) specifically reduced GAPDH signal without a change in TRPM2 staining, although the GAPDH-reduced neurons displayed typically flattened morphology. There was no change in the number of living neurons by either treatment of siRNA. Higher concentration of siTRPM2 was also effective, but non-specific reduction in GAPDH was observed at 3 nM or more (data not shown).

In fura-2-loaded neurons after pretreatment with siTRPM2 or siGAPDH, neither basal $[Ca^{2+}]_i$ concentration nor a small rise in $[Ca^{2+}]_i$ by H_2O_2 in Ca^{2+}-free solution was affected, whereas H_2O_2-induced Ca^{2+} influx was greatly suppressed specifically in neurons treated with siTRPM2 (Fig. 7b). On average, treatment with siTRPM2 caused a significant decrease in the number of stained neurons ($40.2 \pm 2.7\%$ of control, $n = 23$), while the inhibition of H_2O_2-induced Ca^{2+} influx was more apparent (15.2% of control increase, Fig. 7c), implying that H_2O_2-induced Ca^{2+} influx is strongly dependent on TRPM2 expressed in neurons.

Finally, H_2O_2-induced neuronal death was compared under two representative conditions (Fig. 8). The siTRPM2 pretreatment for 3 – 4 days did not affect the number of living neurons before the H_2O_2 treatment. Acute neuronal death by short incubation (20 min) with a high concentration (1 mM) of H_2O_2 was significantly ($P<0.01$) rescued by pretreatment of cultures with siTRPM2. In addition, a long exposure (6 h) to a pathologically relevant concentration (50 μM) of H_2O_2 caused delayed neuronal death, which was also significantly ($P<0.01$) inhibited in siTRPM2-pretreated neurons.

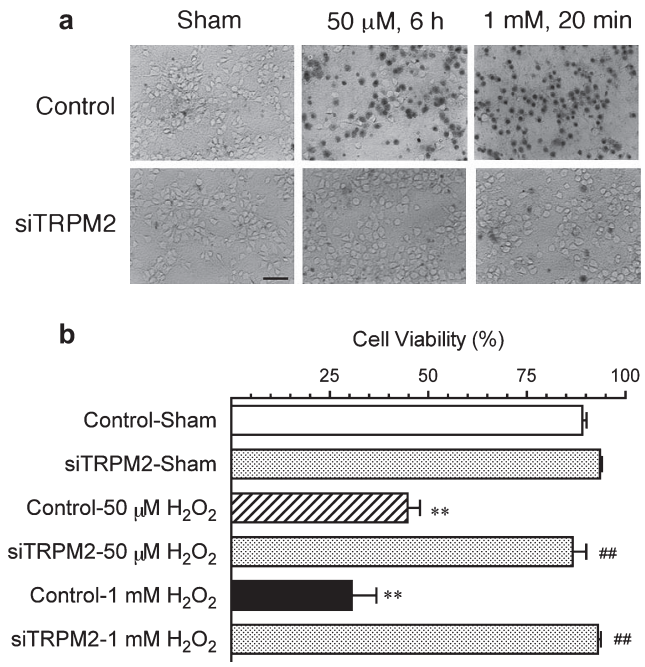

Fig. 8. Rescue from H_2O_2-induced neuronal death by siTRPM2. a: Microphotographs of non-transfected (control) neurons and siTRPM2-transfected neurons after trypan blue staining. Neurons were subjected to sham operation of medium exchange (sham), 1 mM H_2O_2 for 20 min, or 50 μM H_2O_2 for 6 h. Calibration bar = 50 μm. b: Viability was assessed by dividing the number of non-stained cells by the number of total cells. Data are of more than 15 cover slips from 3 experiments. **, $P<0.01$ *vs* Sham group and $^{\#\#}$, $P<0.01$ *vs* Control-H_2O_2-treated group by one-way ANOVA with the *post hoc* Tukey test.

Discussion

The main finding of the present study is that TRPM2 expressed in rat cortical neurons is critically involved in H_2O_2-induced Ca^{2+} influx that causes neuronal death in vitro. We also cloned rat TRPM2 cDNA from rat brain and characterized as ADPR-gated Ca^{2+}-permeable channels that confers H_2O_2-induced cell death by heterologous expression. The nucleotide sequence of rat TRPM2 enables us to manipulate gene expression by RNAi. These findings shed new light on the cascade from the generation of ROS to the degenerative neuronal death.

Overproduction of H_2O_2 molecules in mitochondria contributes to the pathogenesis of many neurodegerative diseases such as Alzheimer's disease, Parkinson's disease, and cerebral ischemia (1, 5, 26). In case of ischemic insult and subsequent reperfusion, concentration of free H_2O_2 in the brain reaches to approximately 100 μM (24), at which H_2O_2 exerts neurotoxic actions on striatal and cortical neurons in vitro (7, 24). The neuronal death by a pathologically relevant concentration of H_2O_2 indicates characteristics of apoptosis with nuclear condensation and DNA laddering (8). However, decrease in ATP level changes the apoptotic cell death to necrotic nature (27). Moreover, H_2O_2 at higher concentrations cause acute necrosis of neural cells (9). Therefore the H_2O_2-induced neuronal death may involve multiple processes leading to apoptotic and necrotic degeneration, depending on the intensity of stimuli, time of exposure, and the cellular environments. In the present study, gene silencing of neuronal TRPM2 was similarly effective to suppress the delayed death by low

concentration of H_2O_2 (50 μM) and the acute death by high concentration of H_2O_2 (1 mM). These results suggest the pivotal role of TRPM2 channels in the cell death pathway downstream of H_2O_2 action.

The primary effects of H_2O_2 may include the oxidation of proteins, such as glutathione, peroxidation of membrane lipids, and breakage and/or base modification of DNA strand (26). In addition, hydroxyl radicals are produced via the Fenton reaction in presence of free Fe^{2+}, which strongly promotes DNA damage. The DNA damage activates the DNA repair enzyme PARP, of which overactivation is considered to be involved in the cell death by oxidative stress (28, 29). Although the mechanism by which PARP activation leads to cell death appears linked to the rapid utilization of NAD^+ during formation of poly-ADPR, recent evidence suggests an important role of poly-ADPR glycohydrolase (PARG) that hydrolyzes poly-ADPR into free ADPR molecules in the oxidative and excitotoxic neuronal death (30). Since inhibitors of PARP prevents H_2O_2-induced opening of TRPM2 channels without affecting direct action of ADPR on TRPM2 channels (31), ADPR may be produced via the PARP – poly-ADPR – PARG pathway in neurons in response to the DNA damage by H_2O_2 or hydroxyl radicals. Alternatively, ADPR can be produced from NAD^+ directly or via cyclic ADPR by catalytic actions of CD38 expressed in neurons and astrocytes (32). This process is also upregulated by nitric oxide via the cyclic GMP pathway (33). Although the detailed mechanism by which ADPR is produced in neurons is unclear, the activation of TRPM2 channels by ADPR leads to irreversible depolarization and unregulated Ca^{2+} entry followed by neuronal death (6, 11). We could not exclude the role of glutamate release and subsequent NMDA receptor activation in the H_2O_2-induced neuronal death, as previously proposed (20). However, heterologous expression of rat TRPM2 is sufficient to induce H_2O_2-induced cell death in HEK cells in which NMDA receptors are not expressed. Considering that cortical neurons also have TRPM7 whose activity is regulated specifically by reactive nitrogen species, such as nitric oxide, and also by H_2O_2 (12), the survival of neurons are differentially or synergistically regulated or threatened, by two TRPM channel-involving systems.

There are several amino acid differences in the Nudix box region of rat TRPM2, as compared to those of human and mouse clones. Based on the structural and mutational analysis of the human NUDT9 molecule that hydrolyzes ADPR (34) with human TRPM2 (35), double mutation from $E^{230}F^{231}$ of NUDT9 to $I^{1405}L^{1406}$ of human TRPM2 (equivalent to $V^{1402}L^{1403}$ of rat TRPM2) causes a decrease in ADPRase activity. Accordingly, it is supposed that the prolonged binding of ADPR, rather than degradation by hydrolysis, is required for the TRPM2 channel opening. Therefore, neighboring double mutations of Arg to Gln at amino acids 1401 and 1404 in rat TRPM2 may be responsible for the higher affinity of rat TRPM2 channels to ADPR by reduced ADPRase activity. The delayed onset of the ADPR-induced TRPM2 channel currents as well as its dependency on extracellular Ca^{2+} concentration suggest the requirement of a rise in $[Ca^{2+}]_i$ for the opening of rat TRPM2 channels, as shown in human and mouse recombinant channels (13) and in H_2O_2-induced Ca^{2+} increase in striatal neurons (10). Delayed onset of H_2O_2-induced Ca^{2+} influx in neurons may involve both metabolic processes producing ADPR and the rise in intracellular Ca^{2+} required for the activation of TRPM2 channels.

In summary, we demonstrate that TRPM2 is abundantly expressed in neurons and plays an important role in the regulation of neuronal survival as well as intracellular Ca^{2+} homeostasis. Since TRPM2 is expressed in neurite extensions as well as cell bodies, TRPM2 may have physiological roles in the synaptic transmission or neurite extension signals by regulating Ca^{2+} and Na^+ entry depending on the cellular redox states. Under pathological conditions, excessive generation of H_2O_2 may cause excess Ca^{2+} entry via TRPM2 channels in addition to other direct actions of H_2O_2 on proteins, lipids, and DNA, while the TRPM2-mediated Ca^{2+} overload is a critical determinant of H_2O_2-induced neuronal death. Thus prevention of Ca^{2+} influx via TRPM2 channels may be effective in rescuing neurons from oxidative stress in vivo. Further research and development of agents that are specifically targeted to the TRPM2 channel may provide a future therapeutic approach for progressive neurodegenerative diseases.

Acknowledgments

This work was supported by Grants-in-Aid from MEXT, Sankyo Foundation of Life Science and Takeda Science Foundation, and by 21st Century COE Program 'Knowledge Information Infrastructure for Genome Science'.

References

1 Jenner P. Oxidative stress in Parkinson's disease. Ann Neurol. 2003;53:S26–S38.
2 Chen Q, Vazquez EJ, Moghaddas S, Hoppel CL, Lesnefsky EJ. Production of reactive oxygen species by mitochondria. J Biol Chem. 2003;278:36027–36031.
3 Abramov AY, Canevari L, Duchen MR. β-Amyloid peptides induce mitochondrial dysfunction and oxidative stress in astro-

cytes and death of neurons through activation of NADPH oxidase. J Neurosci. 2004;24:565–575.
4 Dubinsky JM, Kristal BS, Elizondo-Fournier M. An obligate role for oxygen in the early stages of glutamate-induced, delayed neuronal death. J Neurosci. 1995;15:7071–7078.
5 Banasiak K, Xia Y, Haddad GG. Mechanisms underlying hypoxia-induced neuronal apoptosis. Prog Neurobiol. 2000;62: 215–249.
6 Kristián T, Siesjö BK. Calcium in ischemic cell death. Stroke. 1998;29:705–718.
7 Whittemore ER, Loo DT, Cotman CW. Exposure to hydrogen peroxide induces cell death via apoptosis in cultured rat cortical neurons. NeuroReport. 1994;5:1485–1488.
8 Whittemore ER, Loo DT, Watt JA, Cotman CW. A detailed analysis of hydrogen peroxide-induced cell death in primary neuronal culture. Neuroscience. 1995;67:921–932.
9 Cole KK, Perez-Polo JR. Poly(ADP-ribose) polymerase inhibition prevents both apoptotic-like delayed neuronal death and necrosis after H_2O_2 injury. J Neurochem. 2002;82:19–29.
10 Smith MA, Herson PS, Lee K, Pinnock RD, Ashford MLJ. Hydrogen-peroxide-induced toxicity of rat striatal neurones involves activation of a non-selective cation channel. J Physiol. 2003;547:417–425.
11 Yu SP, Canzoniero LMT, Choi DW. Ion homeostasis and apoptosis. Curr Opin Cell Biol. 2001;13:405–411.
12 Aarts M, Iihara K, Wei W-L, Xiong Z-G, Arundine M, Cerwinski W, et al. A key role for TRPM7 channels in anoxic neuronal death. Cell. 2003;115:863–877.
13 Perraud A-L, Fleig A, Dunn CA, Bagley LA, Launay P, Schmitz C, et al. ADP-ribose gating of the calcium-permeable LTRPC2 channel revealed by Nudix motif homology. Nature. 2001; 411:595–599.
14 Sano Y, Inamura K, Miyake A, Mochizuki S, Yokoi H, Matsushime H, et al. Immunocyte Ca^{2+} influx system mediated by LTRPC2. Science. 2001;293:1327–1330.
15 Nagamine K, Kudoh J, Minoshima S, Kawasaki K, Asakawa S, Ito F, et al. Molecular cloning of a novel putative Ca^{2+} channel protein (TRPC7) highly expressed in brain. Genomics. 1998; 54:124–131.
16 Hara Y, Wakamori M, Ishii M, Maeno E, Nishida M, Toshida T, et al. LTRPC2 Ca^{2+}-permeable channel activated by changes in redox status confers susceptibility to cell death. Mol Cell. 2002;9:163–173.
17 Kraft R, Grimm C, Grosse K, Hoffmann A, Sauerbruch S, Kettenmann H, et al. Hydrogen peroxide and ADP-ribose induce TRPM2-mediated calcium influx and cation currents in microglia. Am J Physiol. 2004;286:C129–C137.
18 Akaike A, Kaneko S, Tanura Y, Nakata N, Shiomi H, Ushikubi F, et al. Prostaglandin E_2 protects cultured cortical neurons against *N*-methyl-D-aspartate receptor-mediated glutamate cytotoxicity. Brain Res. 1994;663:237–243.
19 Hoyt KR, Gallagher AJ, Hastings TG, Reynolds IJ. Characterization of hydrogen peroxide toxicity in cultured rat forebrain neurons. Neurochem Res. 1997;22:333–340.
20 Mailly F, Marin P, Israël M, Glowinski J, Prémont J. Increase in external glutamate and NMDA receptor activation contribute to H_2O_2-induced neuronal apoptosis. J Neurochem. 1999;73:1181–1188.
21 Taguchi R, Nishikawa H, Kume T, Terauchi T, Kaneko S, Katsuki H, et al. Serofendic acid prevents acute glutamate neurotoxicity in cultured cortical neurons. Eur J Pharmacol. 2003;477:195–203.
22 Osakada F, Hashino A, Kume T, Katsuki H, Kaneko S, Akaike A. Neuroprotective effects of α-tocopherol on oxidative stress in rat striatal cultures. Eur J Pharmacol. 2003;465:15–22.
23 Mitchell IJ, Cooper AJ, Griffiths MR. The selective vulnerability of striatopallidal neurons. Prog Neurobiol. 1999;59:691–719.
24 Hyslop PA, Zhang Z, Pearson DV, Phebus LA. Measurement of striatal H_2O_2 by microdialysis following global forebrain ischemia and reperfusion in the rat: correlation with the cytotoxic potential of H_2O_2 in vitro. Brain Res. 1995;671:181–186.
25 McHugh D, Flemming R, Xu S-Z, Perraud A-L, Beech DJ. Critical intracellular Ca^{2+} dependence of transient receptor potential melastatin 2 (TRPM2) cation channel activation. J Biol Chem. 2003;278:11002–11006.
26 Milton NGN. Role of hydrogen peroxide in the aetiology of Alzheimer's disease. Drugs Aging. 2004;21:81–100.
27 Huang F, Vemuri MC, Schneider JS. Modulation of ATP levels alters the mode of hydrogen peroxide-induced cell death in primary cortical cultures: effects of putative neuroprotective agents. Brain Res. 2004;997:79–88.
28 Yu S-W, Wang H, Poitras MF, Coombs C, Bowers WJ, Federoff HJ, et al. Mediation of poly(ADP-ribose) polymerase-1-dependent cell death by apoptosis-inducing factor. Science. 2002;297: 259–263.
29 Pieper AA, Verma A, Zhang J, Snyder SH. Poly(ADP-ribose) polymerase, nitric oxide and cell death. Trends Pharmacol Sci. 1999;20:171–181.
30 Ying W, Sevigny MB, Chen Y, Swanson R. Poly(ADP-ribose) glycohydrolase mediates oxidative and excitotoxic neuronal death. Proc Natl Acad Sci U S A. 2001;98:12227–12232.
31 Fonfria E, Marshall ICB, Benham CD, Boyfield I, Brown JD, Hill K, et al. TRPM2 channel opening in response to oxidative stress is dependent on activation of poly(ADP-ribose) polymerase. Br J Pharmacol. 2004;143:186–192.
32 Yamada M, Mizuguchi M, Otsuka N, Ikeda K, Takahashi H. Ultrastructural localization of CD38 immunoreactivity in rat brain. Brain Res. 1997;756:52–60.
33 Higashida H, Hashii M, Yokoyama S, Hoshi N, Asai K, Kato T. Cyclic ADP-ribose as a potential second messenger for neuronal Ca^{2+} imaging. J Neurochem. 2001;76:321–331.
34 Shen BW, Perraud A-L, Sharenberg A, Stoddard BL. The crystal structure and mutational analysis of human NUDT9. J Mol Biol. 2003;332:385–398.
35 Kühn FJP, Lückhoff A. Sites of the NUDT9-H domain critical for ADP-ribose activation of the cation channel TRPM2. J Biol Chem. 2004;279:46431–46437.